Electronic Supplementary Material (ESI) for Journal of Materials Chemistry C.
This journal is © The Royal Society of Chemistry 2018

Supporting Information

Ultra-stable 2D Layered Methylammonium Cadmium Trihalide Perovskite Photoelectrodes

Hsien-Yi Hsu, Li Ji, Chengxi Zhang, Chun Hong Mak, Rugeng Liu, Tie Wang, Xingli Zou, Shao-Yuan Leu and Edward T. Yu

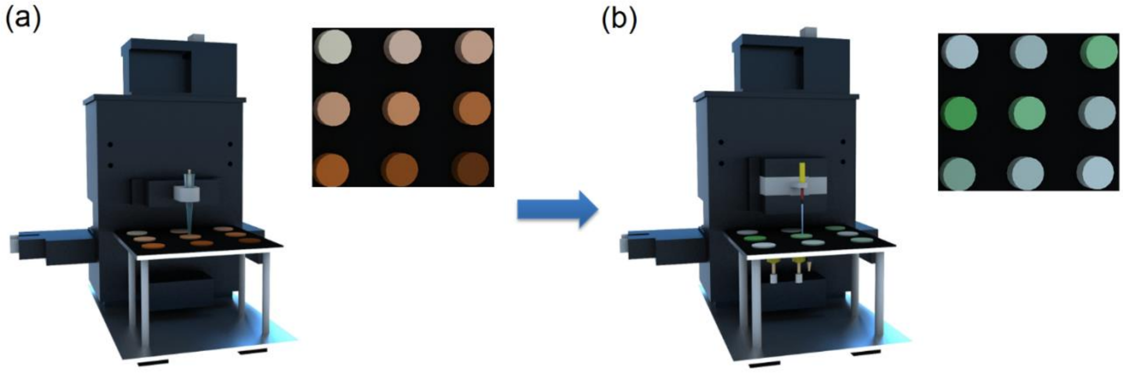

Figure S1. Scanning electrochemical microscopy (SECM) system. (a) Fabrication of perovskite spot array with different compositions using a piezoelectric dispenser (b) Screening analysis on perovskite photoelectrode arrays by SECM.

Table S1. Crystal data and structure refinement for $MACdI_3$.

Empirical Formula	CH_6CdI_3N
Molecular Formula	$MACdI_3$
FW	525.17
T(K)	293
Lattice	Monoclinic
Space group	*P21/n*
a(Å)	9.05
b(Å)	7.048
c(Å)	14.74
α(°)	90
β(°)	90.23
γ(°)	90
V(Å3)	940
Z	4
d_{calc} (g/cm^3)	1.855

μ(mm^{-1})	6.042

Table S2. Crystal data and structure refinement for $(MA)_2CdI_4$.

Empirical Formula	CH_6CdCl_3N
Molecular Formula	$(MA)_2CdI_4$
FW	250.82
T(K)	293
Lattice	Orthorhombic
Space group	*Cmca*
a(Å)	7.391
b(Å)	19.636
c(Å)	7.5139
α(°)	90
β(°)	90
γ(°)	90
V(Å³)	1090.5
Z	1
d_{calc} (g/cm³)	4.583
μ(mm^{-1})	7.977

Table S3. Crystal data and structure refinement for $MACd_3Cl_7{\cdot}3H_2O$.

Empirical Formula	$CH_6Cd_3Cl_9NO$
Molecular Formula	$MACd_3Cl_7{\cdot}3H_2O$
FW	704.32
T(K)	296
Lattice	Monoclinic
Space group	*P21/m*
a(Å)	6.7315
b(Å)	15.9916
c(Å)	6.9266
α(°)	90
β(°)	90.922
γ(°)	90
V(Å³)	745.534
Z	2
d_{calc} (g/cm³)	3.137
μ(mm^{-1})	5.824

Table S4. Photoluminescene decay times (τ_s and τ_{PL}) and corresponding parameters of Cd-based hybrid materials, CD-1, CD-2, CD-3 and CD-4.

Materials	τ_1/ns (α_1)	τ_2/ns (α_2)	τ_{PL} [a]/ns	R^2
CD-1	0.12 (95%)	1.68 (5%)	0.20 ± 0.02	0.99
CD-2	0.21 (87%)	1.70 (13%)	0.40 ± 0.03	0.98
CD-3	0.37 (72%)	1.75 (28%)	0.76 ± 0.01	1.00
CD-4	0.63 (69%)	3.45 (31%)	1.50 ± 0.02	0.99
CD-4, Day 60	0.32 (15%)	0.92 (85%)	0.83 ± 0.01	1.00

[a] $\tau_{PL} = <\tau> = \sum_i \alpha_i \tau$.

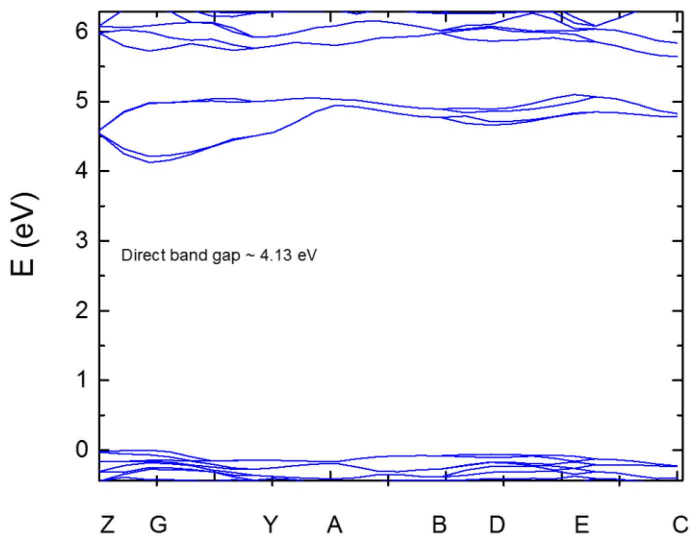

Figure S2. Band structures of $MACdI_3$ calculated by density functional theory.

Table S5. Long-term stability test for hybrid perovskite materials.

Materials	Time (h)	Testing condition: Light/Dark	Temp. (°C)	Atmosphere (RH %)	Sealing	Remaining Photocurrent	Ref.
$(MA)_2CdCl_4$	1440	Light	RT	Air(50)	No	>80%	This work
$MAPbI_3$	230	Light	RT	Air(50)	No	>80 %	This work
$(FAI)_{0.81}(PbI_2)_{0.85}(MABr)_{0.15}(PbBr_2)_{0.15}$	1080	Dark	RT	Air(40)	No	~80%	1
$MAPbI_2Br$	50	Dark	RT	Air	No	~80%	2
$MAPbI_{3-x}Cl_x$(PVK)	55	Light	RT	Air(40~50)	No	~80%	3
$MAPbI_3$	960	Dark	RT	N_2	No	~80%	4
$MAPbI_{3-x}Cl_x$	1000	Light	40	N_2	Yes	~80 %	5
$MAPbI_3$	216	Dark	RT	Air(50)	No	~80%	6
$MAPbI_3$	70	Light	RT	Air(45~50)	No	~70%	7
$MAPbI_3$	130	Dark	RT	Air	No	~80%	8
$CsPbI_2Br$	30	Dark	RT	Air(20)	No	~80%	9
$Cs_{0.925}K_{0.075}PbI_2Br$	125	Dark	RT	Air(20)	No	~80%	9
$CsSnI_3$	336	Dark	RT	Air	No	~80%	10
$FAPbI_3$	360	Dark	RT	Desiccator(15)	No	~70%	11
$CsPbI_2Br$	990	Dark	RT	Glovebox	No	~80%	12
$(FAPbI_3)_{0.85}(MAPbBr_3)_{0.15}$ (LiTFSI)	710	Dark	RT	Air(30)	No	~80%	13

Reference

1. Zhang, F. et al. Isomer‐Pure Bis‐PCBM‐Assisted Crystal Engineering of Perovskite Solar Cells Showing Excellent Efficiency and Stability. *Advanced Materials* **29** (2017).
2. Zhang, M. et al. Stable and Low‐Cost Mesoscopic CH3NH3PbI2Br Perovskite Solar Cells by using a Thin Poly (3‐hexylthiophene) Layer as a Hole Transporter. *Chemistry-A European Journal* **21**, 434-439 (2015).
3. Huang, L. et al. Efficient and stable planar perovskite solar cells with a non-hygroscopic small molecule oxidant doped hole transport layer. *Electrochimica Acta* **196**, 328-336 (2016).
4. Gujar, T.P. & Thelakkat, M. Highly Reproducible and Efficient Perovskite Solar Cells with Extraordinary Stability from Robust CH3NH3PbI3: Towards Large‐Area Devices. *Energy Technology* **4**, 449-457 (2016).
5. Leijtens, T. et al. Overcoming ultraviolet light instability of sensitized TiO 2 with meso-superstructured organometal tri-halide perovskite solar cells. *Nature communications* **4**, 2885 (2013).
6. Christians, J.A., Miranda Herrera, P.A. & Kamat, P.V. Transformation of the excited state and photovoltaic efficiency of CH3NH3PbI3 perovskite upon controlled exposure to humidified air. *Journal of the American Chemical Society* **137**, 1530-1538 (2015).
7. Li, Y. et al. Multifunctional fullerene derivative for interface engineering in perovskite solar cells. *Journal of the American Chemical Society* **137**, 15540-15547 (2015).
8. Kim, J.H. et al. High‐Performance and Environmentally Stable Planar Heterojunction Perovskite Solar Cells Based on a Solution‐Processed Copper‐Doped Nickel Oxide Hole‐Transporting Layer. *Advanced Materials* **27**, 695-701 (2015).
9. Nam, J.K. et al. Potassium incorporation for enhanced performance and stability of fully inorganic cesium lead halide perovskite solar cells. *Nano letters* **17**, 2028-2033 (2017).
10. Yi, C. et al. Entropic stabilization of mixed A-cation ABX 3 metal halide perovskites for high performance perovskite solar cells. *Energy & Environmental Science* **9**, 656-662 (2016).
11. Li, Z. et al. Stabilizing perovskite structures by tuning tolerance factor: formation of formamidinium and cesium lead iodide solid-state alloys. *Chemistry of Materials* **28**, 284-292 (2015).
12. Zeng, Q. et al. Polymer‐Passivated Inorganic Cesium Lead Mixed‐Halide Perovskites for Stable and Efficient Solar Cells with High Open‐Circuit Voltage over 1.3 V. *Advanced Materials* (2018).
13. Qu, J. et al. Improved performance and air stability of perovskite solar cells based on low-cost organic hole-transporting material X60 by incorporating its dicationic salt. *Science China Chemistry* **61**, 172-179 (2018).